# Interfacial Polyelectrolyte-Surfactant Complexes Regulate Escape of Microdroplets Elastically Trapped in Thermotropic Liquid Crystals

Michael Tsuei<sup>1</sup>, Hao Sun<sup>2,3</sup>, Young-Ki Kim<sup>1,4</sup>, Xin Wang<sup>1</sup>, Nathan C. Gianneschi<sup>2\*</sup>, and Nicholas L. Abbott<sup>1\*</sup>

Liquid Crystals, Emulsions, Electrical Double Layer Interactions, Elastic Forces, Polyelectrolyte-Surfactant Complexes.

ABSTRACT: Polyelectrolytes adsorbed at soft interfaces are used in contexts such as materials synthesis, stabilization of emulsions, and control of rheology. Here we explore how polyelectrolyte adsorption to aqueous interfaces of thermotropic liquid crystals (LCs) influences surfactant-stabilized aqueous microdroplets that are elastically trapped within the LC. We find that adsorption of poly(diallyldimethylammonium chloride) (PDDA) to the interface of a nematic phase of 4-cyano-4'-pentylbiphenyl (5CB) triggers the ejection of microdroplets decorated with sodium dodecylsulfate (SDS), consistent with an attractive electrical double layer interaction between the microdroplets and LC interface. The concentration of PDDA that triggers release of the microdroplets (millimolar), however, is three orders of magnitude higher than that which saturates the LC interfacial charge (micromolar). Observation of a transient reorientation of the LC during escape of microdroplets leads us to conclude that complexes of PDDA and SDS form at the LC interface and thereby regulate interfacial charge and microdroplet escape. Poly(sodium 4-styrenesulfonate) (PSS) also triggers escape of dodecyltrimethylammonium bromide (DTAB)-decorated aqueous microdroplets from 5CB with dynamics consistent with the formation of interfacial polyelectrolyte-surfactant complexes. In contrast to PDDA-SDS, however, we do not observe a transient reorientation of the LC when using PSS-DTAB, reflecting weak association of DTAB and PSS and slow kinetics of formation of PSS-DTAB complexes. Our results reveal the central role of polyelectrolyte-surfactant dynamics in regulating the escape of the microdroplets and, more broadly, that LCs offer the basis of a novel probe of the structure and properties of polyelectrolytesurfactant complexes at interfaces. We demonstrate the utility of these new insights by triggering the ejection of microdroplets from LCs using peptide-polymer amphiphiles that switch their net charge upon being processed by enzymes. Overall, our results provide fresh insight into the formation of polyelectrolyte-surfactant complexes at aqueous-LC interfaces and new principles for the design of responsive soft matter.

#### INTRODUCTION

The adsorption of polyelectrolytes from solution provides the basis of a versatile approach for tailoring the interfacial properties of a range of materials. <sup>1-5</sup> For example, control of interfacial charge, <sup>6-8</sup> surface chemical functionality, <sup>9</sup> and surface tension <sup>6, 10, 11</sup> via polyelectrolyte adsorption has been used for the preparation of biocompatible coatings <sup>12-14</sup>, formulating cosmetics <sup>15, 16</sup> and for achieving colloidal stability. <sup>7, 17, 18</sup> Additional control over the properties of surfaces decorated with polyelectrolytes can be achieved through the use of surfactants, which often spontaneously complex with adsorbed polyelectrolytes. <sup>19-31</sup> Past studies have probed polyelectrolyte-surfactant interactions at air-water interfaces <sup>24, 26-28, 30</sup> and oil-water interfaces<sup>2, 21, 32</sup> using methods such as dilational rheology, <sup>33, 34</sup> dynamic light scattering (DLS), <sup>34</sup> surface tensiometry, <sup>11, 35</sup> and

zeta potential measurements. <sup>11, 35 36</sup> In this work, we investigate polyelectrolyte-surfactant interactions at aqueous interfaces of thermotropic liquid crystals (LCs), revealing that formation of the complexes can trigger and regulate the escape of aqueous emulsion droplets trapped within the LC as well as generate LC orientational transitions that depend on the identity of the polyelectrolytes and surfactants within the complexes.

Our focus on LC interfaces is motivated by past observations that the long range ordering of molecules within LCs (e.g., 4-cyano-4'-pentylbiphenyl (5CB), inset in Figure 1a)<sup>37, 38</sup> enables LCs to rapidly reorganize and communicate information across macroscopic distances. These properties of LCs have been used to amplify and transduce molecular-level events at their interfaces into easily visualized and quantifiable changes in optical signals.<sup>39-42</sup> In addition, it was recently shown that surfactant-stabilized aqueous microdroplets (containing bioactive agents

<sup>&</sup>lt;sup>1</sup> Smith School of Chemical and Biomolecular Engineering, Cornell University, Ithaca, NY 14853, USA

<sup>&</sup>lt;sup>2</sup> Department of Chemistry, Materials Science & Engineering and Biomedical Engineering, Northwestern University, Evanston, IL 60208, USA

<sup>&</sup>lt;sup>3</sup> Department of Chemistry and Chemical & Biomedical Engineering, University of New Haven, West Haven, CT 06516, USA

<sup>&</sup>lt;sup>4</sup> Department of Chemical Engineering, Pohang University of Science and Technology, Pohang, Gyengbuk 37673, Korea

such as antimicrobial species), when elastically trapped by either achiral or chiral nematic LCs (see below for additional details), can be triggered to escape from the LCs using chemical and physical stimuli delivered to the LC interface (e.g., shear stresses induced by motion of motile bacteria near the interface).<sup>43</sup> In this paper, we build on these prior results by testing the hypothesis that adsorption of polyelectrolytes onto the aqueous-nematic LC interface can trigger the escape of the microdroplets from the LC when the sign of the charge of the polyelectrolyte is opposite to that of the surfactant used to stabilize the aqueous droplets (i.e., as a consequence of attractive electrical double layer interactions). While this hypothesis is supported by our observations, we found that the transient presence and dynamic properties of polyelectrolyte-surfactant complexes formed at the LC interface played a key role in regulating the escape of the microdroplets.

Several past studies have reported on the interactions of LCs and polyelectrolyte complexes. 44-47 Abbott and Caruso reported that the interactions of lipid-enveloped virus particles with polyelectrolyte-decorated LC interfaces triggered LC ordering transitions that report the presence of the virus.<sup>48</sup> Bera and coworkers reported that alternating deposition of anionic and cationic polyelectrolytes onto the aqueous interface of LC droplets can change the orientation of the LC. 45 They also reported on the interactions of polyelectrolyte-surfactant complexes with LCs, finding that the surfactant concentration required to trigger a change in the orientation of a LC was several orders of magnitude lower than that required for systems containing only surfactant. 49 This result led the authors to conclude that the role of the polyelectrolyte was to concentrate surfactants at the LC interface. In the current study, in the context of understanding how polyelectrolytes can trigger the release of aqueous microdroplets from LCs, we show that the response of a LC to a polyelectrolyte-surfactant complex depends on the identity of both species, revealing in particular that the dynamic properties of surfactant-polyelectrolyte complexes regulate a range of interfacial phenomena at aqueous-LC interfaces (e.g., LC orientations).

#### **EXPERIMENTAL**

Materials. The nematic LC 4-cyano-4'-pentylbiphenyl (5CB) was purchased from HCCH (Jiangsu Hecheng Display Technology Co., Ltd). Poly(diallyldimethylammonium chloride) (PDDA,  $M_w$ <100,000 g/mol), poly(sodium 4-styrenesulfonate) (PSS,  $M_w$ = 70,000 g/mol), sodium dodecyl sulfate (SDS, purity ≥99%) and dodecyltrimethylammonium bromide (DTAB, purity ~99%) were purchased from Sigma Aldrich. Fisherfinest premium grade glass slides were purchased from Fisher Scientific (Pittsburgh, PA). N,N-dimethyl-N-octadecyl-3-aminopropyltrimethoxysilyl chloride (DMOAP) was purchased from Sigma Aldrich. Purification of water (18.2 MΩ cm resistivity at 25 °C) was performed using a Milli-Q water system (Millipore, Bedford, MA, USA).

**Preparation of 20 \mum-Thick LC Films.** 20  $\mu$ m-thick LC films of 5CB were created by pipetting 0.2  $\mu$ L of 5CB into the pores of 75 mesh copper transmission electron microscopy (TEM) grids resting on a DMOAP-functionalized glass substrate. The excess 5CB was removed via capillary action using a 10  $\mu$ L pipette tip to form a flat LC interface.

Preparation of Aqueous Microdroplet-in-LC Emulsions. LC emulsions were prepared as follows. Aqueous solutions of surfactant at concentrations below their CMC ( $C_{\rm SDS}=5$  mM,  $C_{\rm DTAB}=10$  mM) were prepared. The purity of the surfactants was confirmed by measuring the surface tension as a function of surfactant concentration and verifying that there was no minimum in the plot near the critical micelle concentration (see Section S1). The aqueous surfactant solutions were then emulsified into the nematic LC (1.5 v/v% microdroplets in LC) by vortexing for 30 seconds at 1,000 revolutions per minute (rpm), followed by 30 seconds at 2,000 rpm, and 30 seconds at 3,000 rpm

**Preparation of 125 \mum-Thick LC Films.** 125  $\mu$ m-thick films of water-in-LC emulsion were created by pipetting 0.8  $\mu$ L of the emulsion into the pores of 75 mesh copper transmission electron microscopy (TEM) grids resting on a DMOAP-functionalized glass substrate. The film was then directly immersed into the aqueous polyelectrolyte solution.

**Zeta Potential (ζ) Measurements.** LC-in-water emulsions were formed by homogenizing a mixture of 5CB in an aqueous solution comprising polyelectrolyte for 30 s. The LC-in-water emulsion was then diluted in aqueous polyelectrolyte solution (same polyelectrolyte concentration) to match the total surface area of the LC droplets with the LC films (4 mm²) used in our experiments. After allowing 30 min for the sample to equilibrate, the zeta potential on the aqueous side of the aqueous-LC interface was measured using the Malvern Zetasizer Nano instrument.

Measurement of Microdroplet Mass Released. Micrographs were taken over the course of 4 hours. The images were converted to Imagej as a stack, and the extent of escape of microdroplets from the LC was quantified by measuring the total projected area of microdroplets in the LC film at each point in time (microdroplet release was also confirmed visually in real-time). We calculated the mass of microdroplets released into the aqueous bulk from the initial mass loaded  $(0.8 \, \mu g)$  and the fractional release (as determined by imaging).

**Synthesis of Charge Invertible Peptide-Polymers (CIP).** CIP synthesis procedures and characterization are provided in the Supporting Information.

Thermolysin-induced Cleavage of CIPs. 3 mM CIP in aqueous 0.5 mM CaCl $_2$  was prepared. Aqueous thermolysin was then mixed into the CIP mixture to make an aqueous solution comprising 3 mM CIP, 0.5 mM CaCl $_2$ , and 60  $\mu$ M Thermolysin. The mixture was then heated at 55 °C for 12 hours to promote enzymatic cleavage of the CIP.

### **RESULTS AND DISCUSSION**

Colloidal Interactions of Aqueous Microdroplets Elastically Trapped Within LCs. At the outset of this study, we sought to determine whether PDDA adsorption at the aqueous-LC interface would modulate the LC interfacial charge, and subsequently generate electrical double layer interactions that trigger the ejection of aqueous SDS-decorated microdroplets elastically trapped within LC films (Figure 1). We used 5CB in the studies reported in this paper because the aqueous-nematic 5CB interface has been widely studied, <sup>50, 51</sup> and because 5CB forms

a room temperature nematic phase as a single component. First, we verified that PDDA adsorbs to aqueous-LC interfaces by measuring zeta potentials ( $\zeta$ ) of LC microdroplets of 5CB dispersed in aqueous PDDA (see Materials and Methods). In the absence of PDDA ( $C_{PDDA} = 0$ ), we measured zeta potentials of  $-24 \pm 3$  mV (Figure 2a). At  $C_{PDDA} = 6$   $\mu$ M (concentration of PDDA monomers), the LC interfacial charge reversed ( $\zeta_{aq-LC} = 37 \pm 2$  mV), indicating the adsorption of PDDA onto the LC interface. Ultimately, when  $C_{PDDA} > 0.6$  mM, we observed the interfacial charge to saturate with a corresponding zeta potential of  $52 \pm 1$  mV (Figure 2a). This result indicates that at concentrations above 0.6 mM PDDA, there is excess PDDA in the bulk aqueous solution.

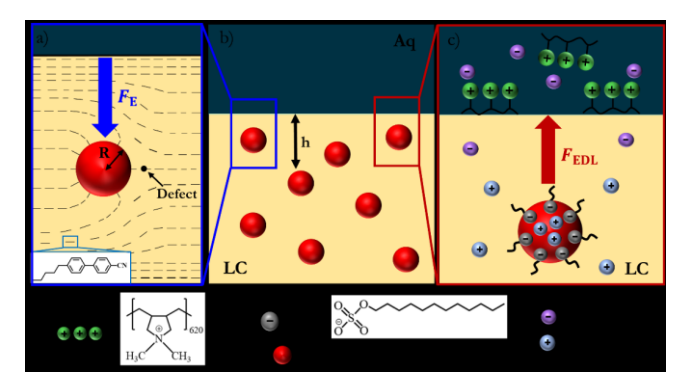


**Figure 1.** (a-c) Schematic illustrations of colloidal interactions of aqueous microdroplets dispersed in a nematic film of 5CB. (a) Elastically trapped microdroplet with radius R in a bulk nematic ( $F_{\rm E}$  represents elastic force between the microdroplet and the interface of the LC to an overlying aqueous phase). (b) Dispersion of microdroplets in LC (h is the distance between the microdroplet and aqueous-LC interface). (c) Electrical double layer interaction ( $F_{\rm EDL}$ ) between the surfactant stabilized aqueous microdroplet (SDS) and cationic polyelectrolyte (PDDA) adsorbed at the aqueous interface of the LC.

Next, we calculated the magnitudes of the colloidal interactions (elastic and electrical double layer) between the dispersed aqueous microdroplets and the LC interface with the overlying aqueous phase. The force acting on the microdroplet due to elastic interactions,  $F_{\rm E}$ ,  $^{43,54}$  was evaluated as

$$F_{\rm E} = -\pi K A^2 B \left[ \frac{R}{h+R} \right]^4 \tag{1}$$

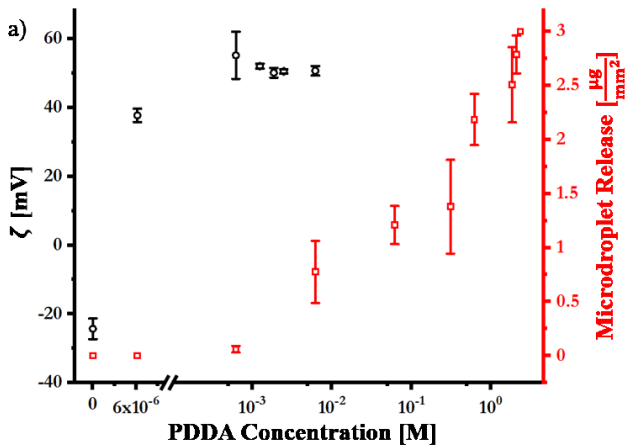
where R is the radius of a microdroplet (Figure 1a), h is the distance between the microdroplet surface and aqueous-LC interface (Figure 1b), K is the elastic constant of the LC, and B is a constant associated with the LC orientation at the aqueous-LC interface, such that B=1/2 for perpendicular (homeotropic) alignment and B=3/4 for tangential (planar) alignment. A is a numerical prefactor that takes the value of 2.04 for droplets with  $R \ge 1$  µm and homeotropic anchoring. The force due to electrical double layer interactions,  $F_{\rm EDL}$  was evaluated as

$$F_{\rm EDL} = -4\pi\varepsilon_0 \varepsilon \kappa R \left(\frac{kT}{e_r}\right)^2 Y_{\rm P} Y_{\rm i} \exp(-\kappa h) \tag{2}$$

where,  $\varepsilon_0$  is the vacuum permittivity,  $\varepsilon$  is the relative permittivity of the electrolyte solution,  $e_c$  is the elementary charge, T is temperature of the system,  $Y_p$  is the effective surface potential

of the microdroplet,  $Y_i$  is the effective surface potential of the aqueous-LC interface, and  $\kappa$  is the Debye screening length of the LC.<sup>55, 56</sup> Here we note that buoyant forces arising from density differences between the aqueous microdroplets and LC ( $\rho_{\text{microdroplet}}$ = 1.00 g/mL;  $\rho_{\text{LC}}$ = 1.01 g/mL) were calculated to be two orders of magnitude smaller than  $F_{\text{E}}$  and  $F_{\text{EDL}}$  when the microdroplets are separated from the LC by distances (h) of a few micrometers or less (see Section S2).

Figure 2b shows the net forces predicted to act on aqueous microdroplets dispersed in LC due to  $F_{\rm EDL}$  and  $F_{\rm E}$  (see Section S3 for details, including values of parameters used in Eq. 1 and 2). When the phase overlying the LC is water ( $\zeta_{\rm aq-LC} = -24 \pm 3$  mV), we predicted that aqueous microdroplets stabilized by SDS will be sequestered within the LC (F < 0, Figure 2b; purple line). In contrast, when PDDA is added to a concentration of  $C_{\rm PDDA} = 0.6$  mM (assuming planar LC alignment), we predicted F to be positive (Figure 2b, blue line), indicating that microdroplets can escape from the LC. Below we test these predictions in experiments.



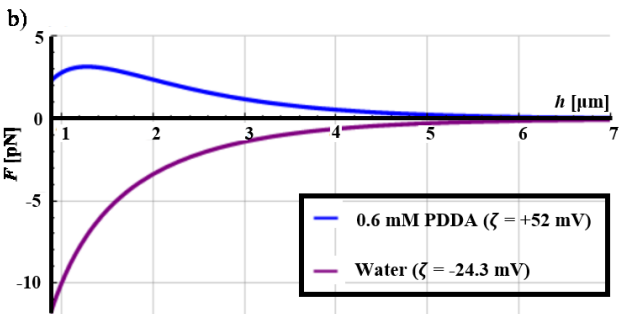


**Figure 2:** (a) Zeta potentials ( $\zeta$ , black circles) measured at interfaces of droplets of nematic 5CB incubated in 0.6 mM PDDA, and mass per unit LC film area of SDS-stabilized microdroplets ejected after 4 hours (red squares) of incubation in aqueous PDDA solutions. (b) Predicted net forces (comprising  $F_{\rm E} + F_{\rm EDL}$ ) acting between SDS-stabilized aqueous microdroplets and LC interface before (purple line) and after adsorption of PDDA (blue line) from the bulk aqueous solution.

**PDDA-Triggered Microdroplet Escape from LCs.** We prepared 125 µm-thick LC films of 5CB containing SDS-stabilized microdroplets (3 µg of microdroplets per square millimeter of LC within the film; diameters of  $3 \pm 2$  µm; see Materials and Methods), and then immersed the films into water ( $C_{PDDA} = 0$ ). We observed the microdroplets to remain trapped in the LC,

consistent with repulsive  $F_E$  and  $F_{EDL}$  acting on the microdroplets near the LC interface (Figure 2a; red square). After addition of PDDA to a concentration of  $C_{PDDA} = 0.6$  mM, however, we observed the escape of  $4 \pm 2 \text{ v/v}\%$  of the microdroplets from the LC within 2.5 minutes of addition of the PDDA (see Materials and Methods). Following this initial release, however, no further escape of microdroplets was observed during an additional 4 hours of incubation of the LC interface against the PDDA solution (Figure 2a; red squares, Section S4). In contrast, for  $C_{PDDA} > 0.6$  mM, conditions under which we measured the LC interfacial charge density to be saturated by PDDA adsorption ( $\zeta_{aq-LC} = 52 \pm 1$  mV; Figure 2a), we measured the rate and extent of escape of microdroplets to increase with  $C_{PDDA}$ such that at  $C_{PDDA} = 2.4$  M all of microdroplets initially in the LC were ejected (Figure 2a; red squares). We verified that aqueous microdroplets ejected from the LC were not coated by a thin LC shell by observing the microdroplets using optical microscopy (side view; bright field and polarized light) following their release into the bulk aqueous phase. While these observations, when combined, are generally consistent with our proposal that PDDA-regulated interfacial charge density can trigger the release of SDS-stabilized microdroplets from the LC (Figure 2b), the need for such high concentrations of PDDA to trigger complete release of microdroplets led us to investigate further the mechanisms by which PDDA influences the escape of the microdroplets.

Mechanisms by which PDDA Triggers Microdroplets Escape from LC. We approached this question of how PDDA influences the escape of SDS-stabilized microdroplets by considering a possible role for colloidal phenomena beyond  $F_{\rm EDL}$ , such as convective flows, <sup>43, 57</sup> osmotic pressure differences (diffusiophoresis), <sup>58, 59</sup> and reorientation of the LC. <sup>54, 60</sup> First, we performed microscopic observations to determine whether convective flows occurred near the LC interface, which would facilitate transport of microdroplets to the aqueous-LC interface and potentially promote their rate of escape from the LC. We determined, however, that adsorption of PDDA at the aqueous-LC interface does not induce convective flows via direct observation of interfaces between aqueous PDDA and LC (see Section S5).

Second, because microdroplet escape was found to depend on  $C_{\rm PDDA}$ , we considered the possible role of osmotic pressure differences between the microdroplets and aqueous bulk. In the experiments described above, the microdroplets contained 5 mM of sodium and 5 mM of dodecyl sulfate ions whereas the bulk aqueous phase contains 1  $\mu$ M of PDDA (0.6 mM of monomer units) along with 0.6 mM of counterions. To determine if an increase in the osmotic pressure of the bulk aqueous phase would impact microdroplet release, we added 10 mM glucose to the aqueous bulk in addition to the PDDA (Section S6). We found, however, that the additional glucose (and thus osmotic pressure difference) did not change the escape of the microdroplets. This result suggests that the microdroplet escape reported in Figure 2a is not influenced by changes in osmotic pressure associated with the addition of PDDA.

Third, we explored the influence of PDDA adsorption on the LC orientation at the aqueous interface. Specifically, we immersed LC films (containing SDS-decorated microdroplets) in aqueous solutions comprising either water (Figure 3a),  $C_{\text{PDDA}} =$ 

60 mM (Figure 3b), or  $C_{PDDA} = 2.4$  M (Figure 3c). In the absence of PDDA (Figure 3a), when viewed between crossed-polarizers over 4 hours, the LC films maintained a bright optical appearance. This appearance is consistent with planar alignment of the LC at the aqueous-LC interface. Additionally, no microdroplets escaped from the LC during the 4 hrs (Figure 3d). While past studies have reported that surfactants can exhibit low solubility in LCs, 61 the former result indicates that any partitioning of SDS into the LC in our experiments is sufficiently low that it does not impact the LC orientation at the aqueous-LC interface. This conclusion regarding the low extent of partitioning of SDS into the LC is further supported by the absence of a change in the nematic-to-isotropic phase transition temperature  $(T_{\rm NI})$  of LC films (no microdroplets) immersed in aqueous 1 mM SDS for 4 hours ( $T_{\rm NI}$  = 35.5 ± 0.1 °C). When combined, these observations indicate that SDS partitioning into the LC does not affect the escape of microdroplets reported in our experiments.

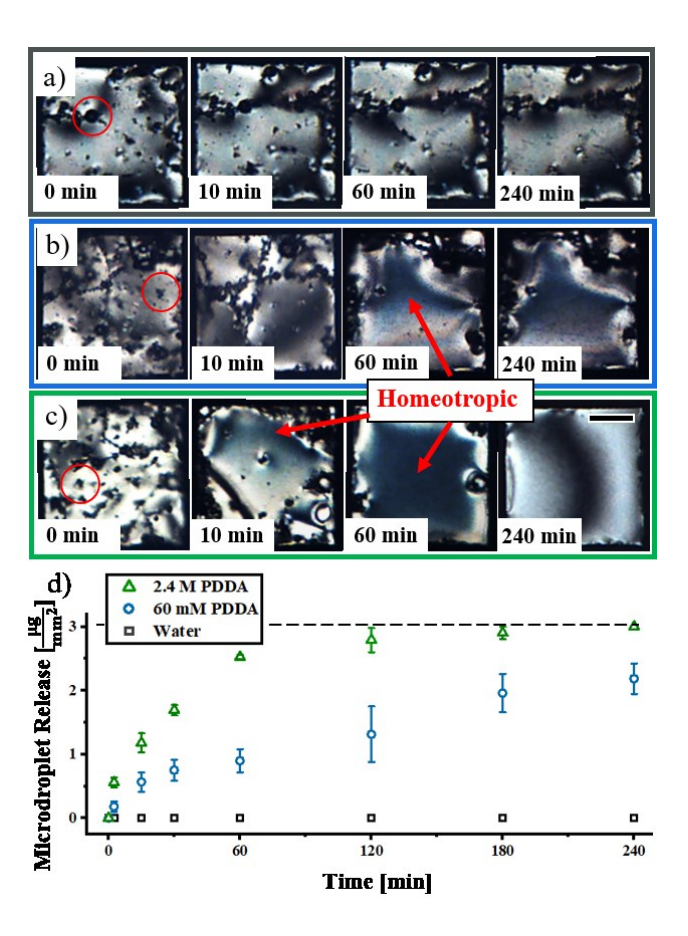


**Figure 3:** (a-c) Sequential optical micrographs (crossed polarizers) of 125 μm-thick LC films containing aqueous 5 mM SDS-decorated microdroplets (example circled in red) that were immersed in aqueous baths of (a) water, (b)  $C_{\text{PDDA}} = 60$  mM, and (c)  $C_{\text{PDDA}} = 2.4$  M. Each image shows the time elapsed since immersion into the PDDA solution. (d) Microdroplets (mass per unit area of LC film) ejected from LC as a function of time. Scale bar is 100 μm. Dashed line represents total mass of microdroplets in LC.

At  $C_{PDDA} = 60$  mM (Figure 3b), we observed the LC film to exhibit a planar LC alignment (consistent with that observed in

water) for approximately 30 mins following contact with the PDDA. Subsequently, we found that localized regions of the LC interface underwent a planar to homeotropic (perpendicular) orientational transition, with the fraction of the surface exhibiting the homeotropic orientation increasing over 4 hrs (Figure 3b). After 24 hrs of incubation with the PDDA, however, the LC was observed to have relaxed back to its initial planar orientation. Accompanying this time-dependent change in LC orientation, we observed release of the aqueous microdroplets, with the initial release occurring during the first 30 mins when the LC was in its initial planar orientation. After 4 hours,  $70 \pm$ 8 v/v% of the microdroplets were measured to have escaped (Figure 3d), with complete release observed after 24 hrs (Figure 3b). At  $C_{PDDA} = 2.4$  M (Figure 3c), we observed the same sequence of states of the system as when using 60 mM of PDDA, but the dynamics of the processes were accelerated. For example, within 4 hrs of exposure to the PDDA, all microdroplets had been released and the LC had reverted to its planar alignment from a transient homeotropic state (Figure 3c,d).

The observations described above lead to three key conclusions. First, microdroplet escape is, in some cases, accompanied by a planar to homeotropic reorientation of the LC (Figure 3b,c). Second, the LC reorientation observed to accompany the escape of microdroplets is transient, indicating that the phenomena underlying the reorientation is dynamic (Figure 3c). Third, the lifetime of the transient homeotropic state of the LC is controlled by the concentration of PDDA in the aqueous bulk. While these results establish that reorientation of the LC can accompany the release of microdroplets, the factors that control the reorientation, and whether or not reorientation is needed for the release of all microdroplets, are not established by these results. These open questions are addressed by the studies reported below.

Additional Observations that Identify the Role of Polyelectrolyte-Surfactant Complexes in Regulating Microdroplet Escape from LCs. Next, we investigated why microdroplet escape was accompanied in some cases by a planar to homeotropic LC reorientation. Because the microdroplets contain anionic surfactant, we hypothesized that microdroplet escape led to the formation of PDDA-SDS complexes at the LC interface. We tested this proposal by immersing 20 µm-thick LC films (without microdroplets) in aqueous solutions of either 60 mM PDDA or 1 µM SDS, or mixtures of 60 mM PDDA and 1 µM SDS. These experiments revealed that LC films immersed in only 60 mM PDDA or 1 µM SDS exhibited planar LC alignment (See Section S7). In contrast, the LC films immersed in aqueous mixtures comprising 60 mM PDDA and 1 µM SDS exhibited homeotropic alignment (See Section S7). These results led us to conclude that the formation of interfacial PDDA-SDS complexes does likely underlie the observation of transient homeotropic orientation of the LC reported above during microdroplet release (Figure 3). The conclusion is also consistent with prior observations that the concentration of SDS required to trigger a radial configuration of a LC droplet can be lowered substantially by the presence of a cationic polyelectrolyte.<sup>49</sup>

Building from our conclusion that the homeotropic state of the LC is due to formation of interfacial complexes of PDDA-SDS, we interpret the transient nature of the homeotropic LC orientation during escape of microdroplets (Figure 3) to indicate that the LC interface is reporting on the dynamic properties of PDDA-SDS complexes (i.e., their rate of formation and disassembly at the interface). Specifically, we propose that upon escape of a microdroplet, a portion of the LC interface is exposed locally to the concentration of SDS in the released microdroplet (5 mM SDS), which leads to PDDA-SDS complex formation at the LC interface and promotes homeotropic LC alignment (Figure 3b,c). Subsequently, as the complex formed at the interface equilibrates with the overlying aqueous PDDA bulk solution (which will contain less than 0.06 µM SDS, i.e., concentration of SDS if all surfactant in the microdroplets is uniformly dissolved in the aqueous phase; see Section S8), the interfacial complex of SDS dissociates and the LC resumes the initial planar LC alignment (Figure 3c). This interpretation is supported by additional observations of LC films (without microdroplets) immersed in mixtures of 60 mM PDDA and 5 mM SDS (upper bound on transient concentration of SDS at the interface, a discussed above), which exhibit homeotropic alignment, and mixtures of 60 mM PDDA and 0.06 µM SDS (upper bound on the equilibrated concentration of SDS at the interface), which exhibit planar alignment (see Section S9).

We interpret the observations in Figure 3 to indicate that the concentration of PDDA in the aqueous bulk controls (i) the amount of SDS that transiently accumulates on the LC interface as PDDA-SDS complexes (as reported by the extent of homeotropic anchoring of LC at the interface), (ii) the lifetimes of the PDDA-SDS complexes formed at the interfaces (duration of time over which the homeotropic LC orientation is observed), and (iii) the final coverage of SDS on the interface (after equilibration). Specifically, this interpretation is supported by our observations that the transient homeotropic state of the LC film (containing microdroplets) immersed in 2.4 M PDDA is much greater in extent (covers a greater fraction of the surface area of the LC film) yet shorter lived than LC films immersed in 60 mM PDDA (Figure 3b and 3c). We propose that the transient increase in SDS concentration at the LC interface with 2.4 M PDDA is driven by the increase in PDDA adsorbed amount. Additionally, our observation that the lifetimes of the PDDA-SDS complexes decrease with increasing PDDA concentration is consistent with the dynamics of competitive binding of SDS with PDDA at the LC interface and PDDA in the aqueous bulk.62 In particular, higher concentrations of PDDA in the aqueous bulk will promote rapid dissociation of SDS from interfacial complexes, and ultimately lead to a low equilibrium coverage of SDS at the LC interface. Finally, our conclusion that the concentration of PDDA in the aqueous bulk controls the amount of SDS that assembles at equilibrium at the PDDAdecorated LC interface is supported by additional experiments. For example, we immersed 20 µm-thick LC films (no microdroplets) in aqueous mixtures comprising 2.4 M PDDA and 1 μM SDS and found that they exhibited planar alignment. In contrast, mixtures of 60 mM PDDA and 1 µM SDS triggered homeotropic LC alignment, consistent with a higher concentration of SDS on the interface (see Section S9).

Figure 4a-c summarizes our overall conclusions regarding the mechanisms by which the formation of the PDDA-SDS complex at the LC interface regulate the release of microdroplets. Upon immersing LC films (containing SDS-stabilized microdroplets) into aqueous solutions of PDDA, PDDA adsorbs onto the LC interface. The initial adsorption of the PDDA does not change the orientation of the LC, but it does change the surface charge density, which leads to an attractive  $F_{\rm EDL}$  (Figure

4a). If the  $F_{\rm EDL}$  is sufficiently large to overcome  $F_{\rm E}$ , microdroplets escape from the LC, as shown by the predictions in Figure 4d (blue line) based on Eq. 1 and 2. This state of the LC interface, which immediately follows the addition of PDDA, leads to the initial release of microdroplets that we observed in experiments at all PDDA concentrations ( $C_{\rm PDDA} \ge 0.6$  mM).

Accompanying this initial release of microdroplets is the release of SDS (5 mM), which then complexes with the PDDA adsorbed at the LC interface to form PDDA-SDS complexes (Figure 4b). The formation of PDDA-SDS complexes is reported by the LC as a planar to homeotropic reorientation of the LC (Figure 3b,c and Figure 4b). Independent measurements of zeta potentials of LC droplets dispersed in aqueous mixtures of PDDA and SDS revealed a decrease in zeta potential with increasing concentration of SDS such that at 5 mM SDS, the LC interface exhibits a net negative charge<sup>63</sup> ( $\zeta = -43 \pm 4$  mV, see Section S10). These results support our conclusion that PDDA-SDS complexes formed at the LC interface. The complexes trigger the reorientation of the LC, and also lower the excess positive charge density at the LC interface. The associated decrease in  $F_{EDL}$  and thus F will lower (or in some cases arrest) the droplet release rate (Figure 4b,d). Subsequently, the rate of release of microdroplets is determined by the rate of dissociation of the SDS from the PDDA-SDS complexes at the LC interface, as the rate of dissociation of the SDS regulates the magnitude of the excess positive charge density at the interface. As discussed above, the rate of dissociation of SDS is dependent on the bulk concentration of PDDA, thus providing a mechanism that regulates the rate of release of the aqueous microdroplets.

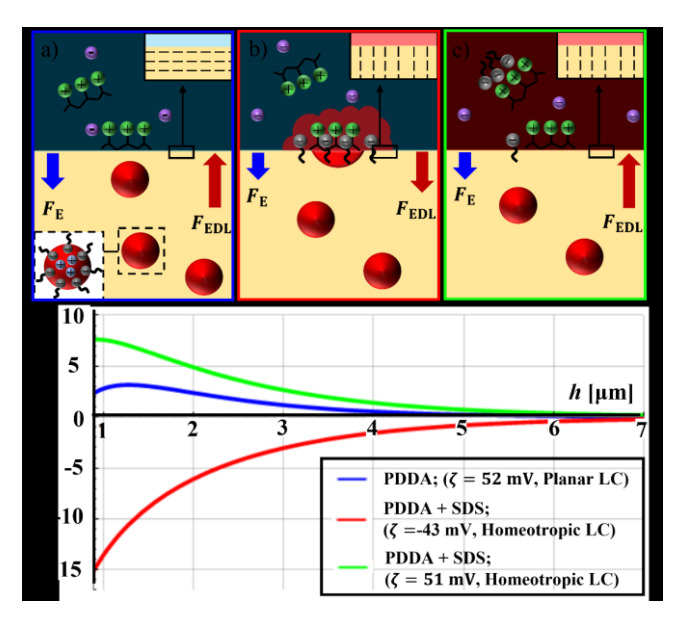


**Figure 4:** Schematic illustrations showing the interfacial processes that accompany PDDA-induced release of aqueous microdroplets stabilized by SDS. (a) PDDA adsorbs at the LC interface to generate an attractive electrical double layer interaction with the SDS-stabilized aqueous microdroplet. (b) The SDS from the released microdroplets form interfacial complexes with the adsorbed PDDA, which lowers the interfacial charge density and lowers the subsequent microdroplet release rate. (c) The SDS in the PDDA-SDS complexes at the LC interface dissociates, thereby partially

restoring LC interfacial charge density, and enabling continued release of microdroplets. (d) Predictions of net forces calculated from Eq. 1 and 2 for the physical situations described in (a-c).

The above-proposed mechanism of release of the microdroplets can be viewed as a type of self-regulated process, as microdroplet release occurs when attractive electrical double layer interactions between the microdroplets and LC interface are sufficiently large, a condition set by the amount of SDS accumulated on the LC interface in complexes with PDDA. What is not established by the experiments and discussion above, however, is the role of the orientational transition of the LC in the mechanism of microdroplet release. Although a change in orientation of the LC (due to formation of PDDA-SDS complexes) will change the elastic barrier that must be overcome for microdroplet release, our previous experiments do not establish whether or not this reorientation is necessary to release all microdroplets from the LC film. Below we address this question in the context of experiments performed using PSS and DTAB.

PSS-Triggered Escape of DTAB-Stabilized Microdroplets from LCs. We explored PSS-triggered release of DTAB-stabilized aqueous microdroplets from nematic 5CB phases because PSS-DTAB complexes have been reported to form interfacial complexes with structures and dynamics that are strikingly different from PDDA-SDS complexes. <sup>24, 64, 65</sup> Whereas PDDA-SDS complexes form largely as a consequence of charge interactions (release of counter ions), <sup>65, 66</sup> the association of PSS and DTAB has been proposed to involve hydrophobic interactions. <sup>67, 68</sup>

We verified that PSS adsorbs to aqueous-nematic 5CB interfaces by measuring zeta potentials of LC droplets dispersed in aqueous PSS ( $C_{PSS}$ ). In particular, we found that the zeta potentials became increasingly negative with increasing PSS concentration, and saturated at  $\zeta = -52 \pm 2$  mV for  $C_{PSS} \ge 3.8$  mM PSS (see Section S11). Next, we experimentally determined whether PSS triggered the escape of DTAB-stabilized microdroplets from LC films and/or changed the LC orientation. We immersed 125 µm-thick LC films containing aqueous microdroplets (stabilized by 10 mM DTAB; total of 3 µg microdroplets per square millimeter of the LC film) into aqueous solutions containing  $C_{PSS} = 1.4 \text{ M}$ . When immersed into the aqueous solution of PSS, after 1 hour, we determined that  $96 \pm 3$ v/v% of the microdroplets escaped from the LC and that after 4 hours all of the microdroplets had escaped the LC (Figure 5a). Significantly, however, and in contrast to PDDA-SDS, during the release of the microdroplets, we observed the LCs to retain a planar alignment throughout the release process (Figure 5a).

The key conclusion that emerges from these experiments is that the reorientation of the LC by transient polyelectrolyte-surfactant complexes is not necessary to trigger microdroplet release. Additionally, however, it leads to the proposal that complexes formed by PDDA-SDS and PSS-DTAB (additional evidence for the formation of PSS-DTAB complexes at the LC interface is presented below) may exert distinct influences on LC orientations. Below we explore this observation further in the context of understanding what properties of interfacial polyelectrolyte-surfactant complexes are reported by LC orientational transitions.

Influence of Interfacial Polyelectrolyte-Surfactant Complexes on LC Orientations. First, we explored how LCs respond to PSS-DTAB complexes at equilibrium. We immersed 20 µm-thick LC films (without microdroplets) in aqueous mixtures comprising different stoichiometric ratios of PSS and DTAB (Figure 5b-e). We found that LCs exhibited homeotropic alignment when contacted with mixtures of DTAB and PSS at stoichiometric ratios (of DTAB:PSS) greater than 1:1 (Figure 5d,e). This contrasts with the LC response to PDDA-SDS complexes, which induce homeotropic alignment of nematic 5CB at stoichiometric ratios (of SDS:PDDA) above 1:10,000 (see Section S9). The 10,000-fold difference in surfactant: polyelectrolyte stoichiometric ratio leading to homeotropic alignment suggests SDS binds to PDDA more strongly than DTAB to PSS. This conclusion is supported by prior studies that have reported higher binding affinities of SDS for PDDA<sup>66, 69</sup> than DTAB for PSS<sup>70</sup> using electrophoretic mobility measurements<sup>66</sup> and isothermal titration calorimetry.<sup>70</sup> We interpret these results to suggests that the absence of a LC orientational transition during microdroplet escape triggered by PSS (Figure 5a) arises, at least in part, due to low interfacial DTAB concentrations (due to weak binding of DTAB to PSS on the LC inter-

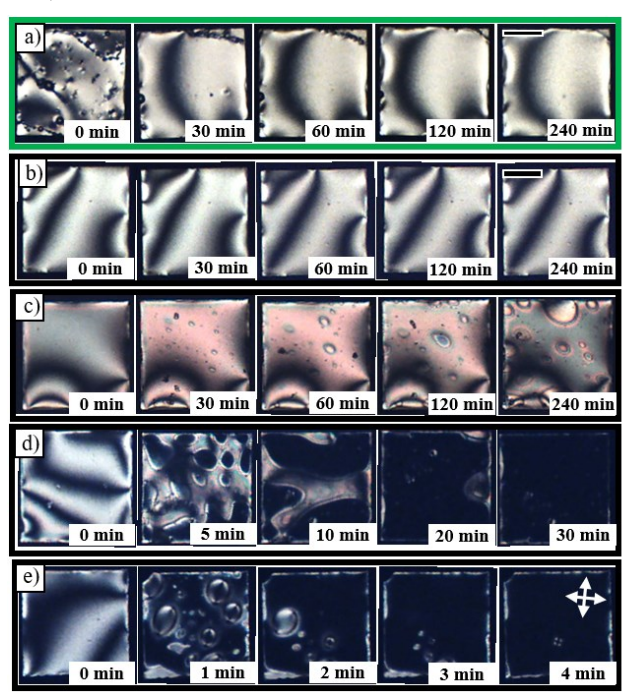


**Figure 5:** (a) Sequential optical micrographs (crossed polarizers) of a 125 μm-thick LC film containing aqueous microdroplets stabilized by 10 mM DTAB. The LC film was immersed (at t = 0 min) into an aqueous solution containing  $C_{\rm PSS} = 1.4$  M. (b-f) Sequential optical micrographs (crossed polars) of 20 μm-thick LC films (no microdroplets) immersed in mixtures of 3.8 mM PSS and either (b) 1 mM, (c) 2.5 mM, (d) 5 mM, or (e) 10 mM DTAB. Scale bars are 100 μm.

Second, we explored the dynamics of formation of PSS and DTAB complexes at the LC interface. We found that LC films immersed into PSS and DTAB solutions (3.8 mM PSS and 5-10 mM DTAB) exhibited orientations that evolved over a duration of mins to hours, finally ending in a homeotropic orienta-

tion (Figure 5d,e). This result suggests that the dynamics of formation of PSS-DTAB complexes are slow, a conclusion that is supported by dilational rheology of PSS-DTAB co-adsorption at air-water interfaces. 65, 71, 72 Our conclusion that LCs can report on the dynamics of formation of polyelectrolyte-surfactant complexes at interfaces is reinforced by our observations that, in contrast to PSS-DTAB, PDDA-SDS can trigger LCs to assume a homeotropic orientation on time-scales of seconds to minutes (e.g., with 3 mM PDDA and SDS). Prior measurements based on ellipsometry and dynamic surface tensiometry reached similar conclusions regarding the dynamics of formation of PDDA-SDS complexes at air-water interfaces.<sup>27</sup> Additional insights into the distinct dynamics of formation of DTAB:PSS and SDS:PDDA complexes can be obtained from studies based on videointerferometry<sup>73, 74</sup> and neutron reflectometry,<sup>65</sup> both which suggest that PSS and DTAB forms viscous multilayers (microgels)<sup>65</sup> at interfaces while PDDA and SDS form compact monolayers. 65, 66 Overall, these observations by us and others, when combined, suggest that a second factor underlying the absence of homeotropic LC orientations during microdroplet release using PSS-DTAB is the slow kinetics of formation of the PSS-DTAB complexes (in contrast, SDS-PDDA complexes form quickly). That is, the DTAB diffuses into the bulk aqueous solution before complexes with PSS can form at the LC interface to change the LC orientation.

Third, we observed patterned orientational domains of LC to form at specific stoichiometric ratios of DTAB to PSS. In particular, as shown in Figure 5c), we found that at stoichiometric ratios (of DTAB:PSS) of 2:3, the LC exhibited tilted optical domains (determined by measurement of the optical retardance using a compensator;  $\theta_{\text{domain}} = 14 \pm 6^{\circ}$  from the surface normal) surrounded by continuous LC regions with a planar alignment (Figure 5c). The tilted domains coalesced and grew in size over time, but were still observed as distinct domains after 48 hrs of equilibration. Because PSS induces planar alignment and DTAB induces homeotropic LC alignment (see Section S12), these observations suggest that mixtures of DTAB and PSS phase separate into DTAB-rich and DTAB-lean domains at the LC interface. 75-78 This observation may be connected to past studies using ellipsometry that have reported formation of micrometer-scale domains (aggregates) at air-water interfaces at stoichiometric ratios of DTAB to PSS similar to those used in our study at LC interfaces. 65, 79 At stoichiometric ratios above 1:1 (Figure 5d,e), we observed the LCs to exhibit a discontinuous transition from planar to homeotropic alignment (patterned homeotropic and planar domains), providing further support for the proposed formation of micrometer-sized domains rich in DTAB. This contrasts with the LC response to PDDA-SDS which, at all stoichiometric ratios of SDS and PDDA investigated in our experiments, involved a transition from planar to a homeotropic orientation via a continuous change in tilt angle (see Section S13). Prior studies of PDDA-SDS at air-water interfaces have also reported the absence of domain structures (uniform, compact monolayers).65,66

Multifunctional LC-based Triggered Release Systems. The results above establish an understanding of how the adsorption of polyelectrolytes at LC interfaces can trigger the release of surfactant-stabilized aqueous microdroplets within the LC. To illustrate how this understanding can be exploited to create LC

systems that can be triggered to release their contents using enzymes, we designed a charge-invertible cationic cleavable peptide-polymer amphiphile (see Materials and Methods and Supporting Information), hereafter, named CIP(+), that undergoes charge reversal via thermolysin-induced cleavage of its peptide functional group to become the anionic peptide-polymer amphiphile, CIP(-) (Figure 6a,b; see Supporting Information for details). We verified the cleavage of CIP(+) in aqueous solution via transmission electron microscopy (TEM; Figure 6c,f), which showed the formation of assemblies between CIP(-) and the cleaved peptide following enzymatic cleavage (Figure 6f).

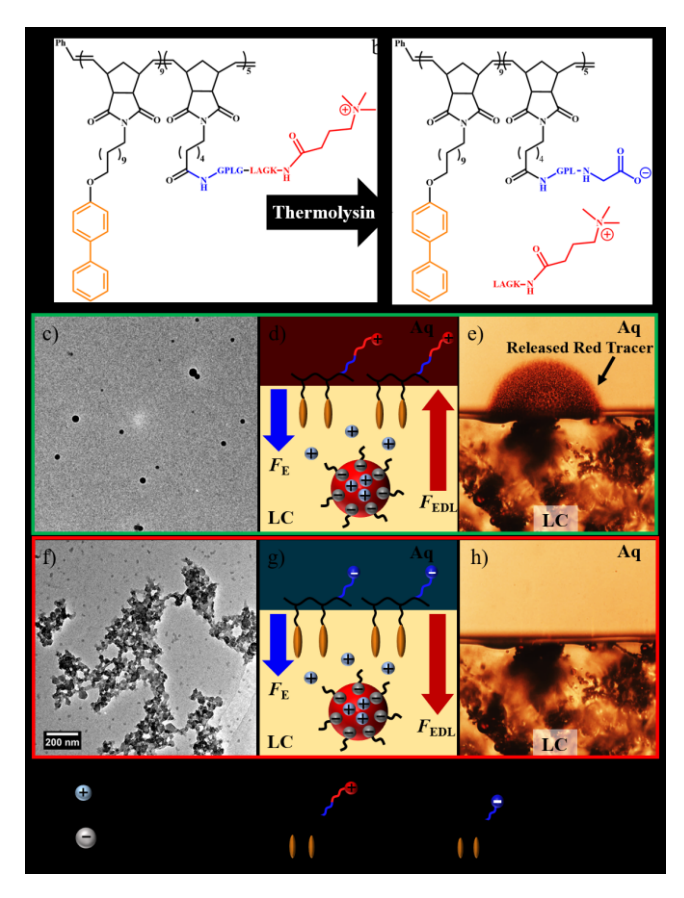


**Figure 6:** (a,b) Molecular structures of (a) pre-cleaved CIP(+) and (b) post-cleaved CIP(-). (c,f) TEM images of aqueous bulk comprising (c) CIP(+) and (f) CIP(-)-cleaved peptide coacervate. (d,g) Schematic illustrations of LC emulsions containing aqueous microdroplets stabilized by SDS in contact with aqueous solutions comprising (d) CIP(+) and (g) CIP(-). (e,h) Corresponding bright field micrographs showing (e) release of tracer-doped microdroplets for LC interfaces contacting aqueous 3 mM CIP(+) and (h) no release of microdroplets for 3 mM CIP(-)-decorated LC interfaces.

The design features of CIP(+), which comprise two repeating blocks (A and B), are as follows. The A block features a linker unit that makes up the backbone of the polyelectrolyte and is conjugated to an 11-carbon aliphatic chain and a biphenyl group that promotes adsorption of the polyelectrolyte at the LC interface. The B block features a linker unit conjugated to a 5-carbon aliphatic chain and a thermolysin-cleavable cationic polypeptide functional group that leads to charging of the LC in-

terface. We verified that CIP(+) and CIP(-) spontaneously adsorb at and charged LC interfaces by dispersing LC droplets in aqueous solutions comprising either CIP(+) or pre-cleaved CIP(-) and measuring zeta potentials at the LC droplet interfaces. Zeta potential measurements revealed that CIP(+)-is characterized by  $+46 \pm 1$  mV, whereas CIP(-) adsorbed at LC interfaces led to a zeta potential of  $-45 \pm 2$  mV. Guided by these zeta potential measurements, we used Eq. 1 and 2 to predict the colloidal interactions of SDS-stabilized aqueous microdroplets within the LC with CIP-decorated LC interfaces. These calculations revealed that CIP(+) generated a net positive F, while CIP(-) generated a negative F, leading us to predict that only CIP(+) would trigger microdroplet escape from the LC (see Section S14). To test these predictions, LC films containing elastically-trapped aqueous microdroplets (5 mM SDS and red tracer) were contacted with bulk aqueous solutions comprising either CIP(+) (Figure 6d,e) or pre-cleaved CIP(-) (Figure 6g,h). We observed release of the SDS-stabilized aqueous microdroplets when using CIP(+) (Figure 6e) but not when using CIP(-) (Figure 6h). This result supports our conclusions that electrical double layer interactions between adsorbed polyelectrolytes and surfactant-stabilized droplets, here controlled by enzymatic processing of the polyelectrolyte, can be used to trigger the release of surfactant-decorated microdroplets from the

#### CONCLUSIONS

A key finding reported in this paper is that adsorption of polyelectrolytes at aqueous interfaces of LCs can be used to trigger the release of surfactant-stabilized aqueous microdroplets dispersed within the LC. Specifically, we found that adsorption of PDDA at LC interfaces triggers the escape of SDS-decorated microdroplets from LCs via an attractive electrical double layer interaction. Additionally, however, we found that interfacial complexes formed between the polyelectrolytes and surfactants released from the microdroplets play a central role in regulating the rate of release of the microdroplets. For example, we found that PDDA aqueous bulk concentration controls the dynamics of PDDA-SDS assembly and disassembly at the LC interface, thereby regulating the rate of escape of the aqueous microdroplets from the LC. While similar microdroplet release dynamics were observed when using PSS and DTAB-stabilized aqueous microdroplets, we observed that interfacial complexes of PSS-DTAB and PDDA-SDS formed during the release process exerted distinct influences on the orientational ordering of the LC. These observations led us to conclude that the orientational behavior of LCs provides the basis of a novel probe of the dynamic properties of polyelectrolytesurfactant complexes at interfaces.

The observations presented in our paper identify a number of opportunities for further investigation. For example, prior studies have reported gelation of polyelectrolytes by surfactants, 80 and the role of gels so-formed on the LC response has not been explored. We have also not yet explored the effect of the order of addition of polyelectrolytes and surfactants on the LC response to polyelectrolyte-surfactant complexation at the aqueous-LC interface. 66 More broadly, the experimental system reported in our paper appears well-suited for characterization of the non-equilibrium interfacial states of surfactants and polyelectrolytes. Additionally, LC mediated interactions between

microdroplets lead to the chaining of microdroplets within the LC; how this chaining impacts the release of microdroplets has not been investigated. Finally, a wide range of polyelectrolytes are found in biological systems, such as DNA, RNA, and polyphosphates, and the results of this study suggest that they could be used to trigger the release of microdroplets. We envisage investigations, for example, in which aqueous microdroplets are loaded with enzymes that, upon release, process the degradation of the adsorbed polyelectrolytes to regulate further release of the protein. Overall, the results reported in this paper provide the basis of general and versatile design rules for the creation of responsive soft matter.

#### ASSOCIATED CONTENT

#### **Supporting Information**

Surface Tension as a Function of SDS Concentration (Section S1); Microdroplet Buoyancy in LC (Section S2); Calculation of Elastic and Electrical Double Layer Interactions (Section S3); LC Emulsions Immersed in Aqueous 0.6 mM PDDA (Section S4); Testing for Convective Flow at Aqueous-LC Interfaces (Section S5); Role of Diffusiophoresis in Microdroplet Escape (Section S6); PDDA-SDS Complex-Induced LC Reorientation (Section S7); Release of a Tracer/SDS-Loaded Microdroplet into the Aqueous Bulk (Section S8); Role of PDDA Concentration on LC Response to PDDA-SDS Complexes (Section S9); Zeta Potentials of LC Droplets in Aqueous Mixtures PDDA and SDS (Section S10); Zeta Potentials of LC Droplets in Aqueous PSS (Section S11); LC Response to PSS and DTAB (Section S12); Dynamics of LC Response to PDDA-SDS Complexation (Section S13); Net Force Between CIP-Decorated LC Interfaces and Microdroplets (Section S14); Materials & Methods (Section S15).

#### **AUTHOR INFORMATION**

Corresponding Authors

E-mail: nla 34 @ cornell.edu, nathan.gianneschi@northwestern.edu

#### ACKNOWLEDGMENT

We acknowledge support of this research from the Army Research Office through W911NF-15-1-0568 and W911NF-17-1-0575.

#### REFERENCES

- 1. Kang, T.; Banquy, X.; Heo, J.; Lim, C.; Lynd, N. A.; Lundberg, P.; Oh, D. X.; Lee, H.-K.; Hong, Y.-K.; Hwang, D. S.; Waite, J. H.; Israelachvili, J. N.; Hawker, C. J., Mussel-Inspired Anchoring of Polymer Loops That Provide Superior Surface Lubrication And Antifouling Properties. *ACS Nano* **2016**, *10* (1), 930-937.
- 2. Zaibudeen, A. W.; Philip, J., Behavior of a Strong Polyelectrolyte, Poly(Diallyldimethylammonium Chloride) Physisorbed at Oil-Water Interface Under Different Environments: A Comparison with a Weak Polyelectrolyte. *Colloids Surf.* **2018**, 550, 209-221.
- 3. Murray, B. S., Rheological Properties of Protein Films. *Curr. Opin. Colloid Interface Sci.* **2011**, *16* (1), 27-35.

- 4. Dickinson, E., Interfacial Interactions and the Stability of Oil-in-Water Emulsions. *Pure Appl. Chem.* **1992**, *64* (11), 1721-1724.
- 5. Riley, J. K.; Matyjaszewski, K.; Tilton, R. D., Friction and Adhesion Control Between Adsorbed Layers of Polyelectrolyte Brush-Grafted nanoparticles via pH-Triggered Bridging Interactions. *J. Colloid Interface Sci.* **2018**, *526*, 114-123.
- 6. Monteillet, H.; Hagemans, F.; Sprakel, J., Charge-driven Coassembly of Polyelectrolytes Across Oil-Water Interfaces. *Soft Matter* **2013**, *9* (47), 11270-11275.
- 7. Yap, H. P.; Quinn, J. F.; Ng, S. M.; Cho, J.; Caruso, F., Colloid Surface Engineering via Deposition of Multilayered Thin Films from Polyelectrolyte Blend Solutions. *Langmuir* **2005**, *21* (10), 4328-4333.
- 8. Szilagyi, I.; Trefalt, G.; Tiraferri, A.; Maroni, P.; Borkovec, M., Polyelectrolyte Adsorption, Interparticle Forces, and Colloidal Aggregation. *Soft Matter* **2014**, *10*, 2479-2502.
- 9. Beaman, D. K.; Robertson, E. J.; Richmond, G. L., Ordered Polyelectrolyte Assembly at the Oil-Water Interface. *PNAS* **2011**, *109* (9), 3226-3231.
- 10. Lam, R. S. H.; Nickerson, M. T., Food Proteins: A Review on their Emulsifying Properties Using a Structure-Function Approach. *Food Chem.* **2013**, *141* (2), 975-984.
- 11. Rodriguez, A. M. B.; Binks, B. P.; Sekine, T., Novel Stabilisation of Emulsions by Soft Particles: Polyelectrolyte Complexes. *Faraday Discuss.* **2016**, *191*.
- 12. Shenoy, D. B.; Antipov, A. A.; Sukhorukov, G. B.; Mohwald, H., Layer-by-Layer Engineering of Biocompatible, Decomposable Core-Shell Structures. *Macromolecules* **2003**, *4* (2), 265-272.
- 13. Kenausis, G. L.; Voros, J.; Elbert, D. L.; Huang, N.; Hofer, R.; Ruiz-Taylor, L.; Textor, M.; Hubbell, J. A.; Spencer, N. D., Poly(L-lysine)-g-Poly(ethylene glycol) Layers on Metal Oxide Surfaces: Attachment Mechanism and Effects of Polymer Architecture on Resistance to Protein Adsorption. *J. Phys. Chem. B.* **2000**, *104* (14), 3298-3309.
- 14. Zhou, J.; Romero, G.; Rojas, E.; Ma, L.; Moya, S.; Gao, C., Layer by Layer Chitosan/Alginate Coatings on Poly(lactide-coglycolide) Nanoparticles for Antifouling Protection and Folic Acid Binding to Achieve Selective Cell Targeting. *J. Colloid Interface Sci.* **2010**, *345* (2), 241-247.
- 15. Xie, A. F.; Granick, S., Phospholipid Membranes as Substrates for Polymer Adsorption. *Nat. Mater.* **2002**, *1*, 129-133.
- 16. Guzman, E.; Ortega, F.; Baghdadli, N.; Cazeneuve, C.; Luengo, G. S.; Rubio, R. G., Adsorption of Conditioning Polymers on Solid Substrates with Different Charge Density. *ACS Appl. Mater. Interfaces* **2011**, *3* (8), 3181-3188.
- 17. Phenrat, T.; Saleh, N.; Sirk, K.; Kim, H.-J.; Tilton, R. D.; Lowry, G. V., Stabilization of Aqueous Nanoscale Zerovalent Iron Dispersions by Anionic Polyelectrolytes: Adsorbed Anionic Polyelectrolyte Layer Properties and their Effect on Aggregation and Sedimentation. *J. Nanopart. Res.* **2007**, *10*, 795-814.
- 18. Bremmell, K. E.; Jameson, G. J.; Biggs, S., Polyelectrolyte Adsorption at the Solid/Liquid Interface: Interaction Forces and Stability. *Colloids Surf.* **1998**, *139* (2), 199-211.
- 19. Lee, J.; Moroi, Y., Binding of Sodium Dodecyl Sulfate to a Cationic Polymer. *Bull. Chem. Soc. Jpn.* **2003**, *76* (11), 2099-2102. 20. Szczepanowicz, K.; Bazylinska, U.; Pietkiewicz, J.; Szyk-Warszynska, L.; Wilk, K. A.; Warszynski, P., Biocompatible Long-sustained Release Oil-Core Polyelectrolyte Nanocarriers: From Controlling Physical State and Stability to Biological Impact. *Adv. Colloid Interface Sci.* **2015**, *222*, 678-691.
- 21. Duner, G.; Kim, M.; Tilton, R. D.; Garoff, S.; Przybycien, T. M., Effect of Polyelectrolyte-surfactant Complexation on Marangoni Transport at a Liquid-Liquid Interface. *J. Colloid Interface Sci.* **2016**, *467*, 105-114.

- 22. Abraham, A.; Kardos, A.; Mezei, A.; Campbell, R. A.; Varga, I., Effects of Ionic Strength on the Surface Tension and Nonequilibrium Interfacial Characteristics of Poly(sodium styrenesulfonate)/Dodecyltrimethylammonium Bromide Mixtures. *Langmuir* **2014**, *30*, 4970-4979.
- 23. Ermakova, T. B.; Sergeeva, I. P.; Anuchkina, A. D.; Sobolev, V. D.; Churaev, N. V., Electrokinetic Study of Layer-by-Layer Polyelectrolyte and Surfactant Adsorbed Layers. *Progr. Colloid Polym. Sci.* **2006**, *132*, 95-101.
- 24. Noskov, B. A.; Loglio, G.; Miller, R., Interaction Between Sodium Poly(styrene sulfonate) and Dodecyltrimethylammonium Bromide at the Air/Water Interface. *Mendeleev Commun.* **2005**, *15* (2), 63-65.
- 25. Langevin, D., Polymer-surfactant Mono and Bilayers. *Rev. inst. Fr. Pet.* **1997**, *52* (2), 109-115.
- 26. Llamas, S.; Fernandez-Pena, L.; Akanno, A.; Guzman, E.; Ortega, V.; Ortega, F.; Csaky, A. G.; Campbell, R. A.; Rubio, R. G., Towards Understanding the Behavior of Polyelectrolyte-Surfactant Mixtures at the Water/Vapor Interface Closer to Technologically-relevant conditions. *Phys. Cheme. Chem. Phys.* **2018**, *20*, 1395-1407.
- 27. Campbell, R. A.; Arteta, M. Y.; Angus-Smyth, A.; Nylander, T.; Noskov, B. A.; Varga, I., Direct Impact of Nonequilibrium Aggregates on the Structure and Morphology of PDADMAC/SDS Layers at the Air/Water Interface. *Langmuir* 2014, 30, 8664-8674. 28. Sharipova, A.; Aidarova, S.; Fainerman, V. B.; Stocco, A.; Cernoch, P.; Miller, R., Dynamics of Adsorption of Polyallylamine Hydrochloride/Sodium Dodecyl Sulphate at Water/Air and Water/Hexane Interfaces. *Colloids Surf.* 2011, 391, 112-118.
- 29. Almgren, M.; Hansson, P.; Mukhtar, E.; Stam, J. v., Aggregation of Alkyltrimethylammonium Surfactants in Aqueous Poly(styrenesulfonate) Solutions. *Langmuir* **1992**, *8*, 2405-2412.
- 30. Akanno, A.; Guzman, E.; Fernandez-Pena, L.; Ortega, F.; Rubio, R. G., Surfactant-like Behavior for the Adsorption of Mixtures of a Polycation and Two Different Zwitterionic Surfactants at the Water/Vapor Interface. *Molecules* **2019**, *24*, 3442-3458.
- 31. Tangso, K. J.; Lindberg, S.; Hartley, P. G.; Knott, R.; Spicer, P.; Boyd, B. J., Formation of Liquid-Crystalline Structures in the Bile Salt-Chitosan System and Triggered Release from Lamellar Phase Bile-Chitosan Capsules. *ACS Appl. Mater. Interfaces* **2014**, *6* (15), 12363-12371.
- 32. Schabes, B. K.; Hopkins, E. J.; Richmond, G. L., Molecular Interactions Leading to the Coadsorption of Surfactant Dodecyltrimethylammonium Bromide and Poly(styrenesulfonate) at the Oil/Water Interface. *Langmuir* **2019**, *35*, 7268-7276.
- 33. Sharipova, A.; Aidarova, S.; Mucic, N.; Miller, R., Dilational Rheology of Polymer/Surfactant Mixtures at Water/Hexane Interface. *Colloids Surf.* **2011**, *391* (1-3), 130-134.
- 34. Kong, L.; Cao, M.; Hai, M., Investigation on the Interaction between Sodium Dodecyl Sulfate and Cationic Polymer by Dynamic Light Scattering, Rheological, and Conductivity Measurements. *J. Chem. Eng. Data* **2007**, *52* (3), 721-726.
- 35. Sharipova, A. A.; Aidarova, S. B.; Grigoriev, D.; Mutalieva, B.; Madibekova, G.; Tleuova, A.; Miller, R., Polymer-surfactant complexes for microencapsulation of vitamin E and its release. *Colloids Surf. B: Biointerfaces* **2016**, *137*, 152-157.
- 36. Li, Y.; Guo, Y.; Xu, G.; Wang, Z.; Bao, M.; Sun, N., Dissipative Particle Simulation on the Properties of the Oil/Water/Surfactant System in the Absence and Presence of Polymer. *Mol. Simul.* **2013**, *39* (4), 299-308.
- 37. Kleman, M.; Lavrentovich, O. D., Soft Matter Physics: An Introduction. *Springer: New York*, **2003**; pp 83-86.

- 38. Gennes, P. G. d.; Prost, J., The Physics of Liquid Crystals 2nd ed. *Clarendon Press; Oxford University Press: Oxford New York*, **1993**; pp 10-13,
- 39. Popov, P.; Mann, E. K.; Jakli, A., Thermotropic Liquid Crystal Films for Biosensors and Beyond. *J. Mater. Chem. B* **2017**, *5* (26), 5061-5078.
- 40. Bukusoglu, E.; Pantoja, M. B.; Mushenheim, P. C.; Wang, X. G.; Abbott, N. L., Design of Responsive and Active (Soft) Materials Using Liquid Crystals. *Annu. Rev. Chem. Biomol.* **2016**, 7, 163-196.
- 41. Carlton, R. J.; Hunter, J. T.; Miller, D. S.; Abbasi, R.; Mushenheim, P. C.; Tan, L. N.; Abbott, N. L., Chemical and Biological Sensing Using Liquid Crystals. *Liq. Cryst. Rev.* **2013**, *1* (1), 29-51.
- 42. Miller, D. S.; Wang, X. G.; Abbott, N. L., Design of Functional Materials Based on Liquid Crystalline Droplets. *Chem. Mater.* **2014**, *26* (1), 496-506.
- 43. Kim, Y.-K.; Wang, X.; Mondkar, P.; Bukusoglu, E.; Abbott, N. L., Self-reporting and Self-regulating Liquid Crystals. *Nature* **2018**, *557*, 539-544.
- 44. Kinsinger, M. I.; Buck, M. E.; Campos, F.; Lynn, D. M.; Abbott, N. L., Dynamic Ordering Transitions of Liquid Crystals Driven by Interfacial Complexes Formed Between Polyanions and Amphiphilic Polyamines. *Langmuir* **2008**, *24* (23), 13231-13236.
- 45. Zou, J.; Bera, T.; Davis, A. A.; Liang, W.; Fang, J., Director Configuration Transitions of Polyelectroltye Coated Liquid-Crystal Droplets. *J. Phys. Chem. B.* **2011**, *115* (29), 8970-8974.
- 46. Price, A. D.; Schwartz, D. K., DNA Hybridization-Induced Reorientation of Liquid Crystal Anchoring at the Nematic Liquid Crystal/Aqueous Interface. *JACS* **2008**, *130* (26), 8188-8194.
- 47. McUmber, A. C.; Noonan, P. S.; Schwartz, D. K., Surfactant-DNA Interactions at the Liquid Crystal-Aqueous Interface. *Soft Matter* **2012**, *8* (16), 4335-4342.
- 48. Sivakumar, S.; Wark, K. L.; Gupta, J. K.; Abbott, N. L.; Caruso, F., Liquid Crystal Emulsions as the Basis of Biological Sensors for the Optical Detection of Bacteria and Viruses. *Adv Funct. Mater.* **2009**, *19*, 2260-2265.
- 49. Bera, T.; Fang, J., Interaction of Surfactants and Polyelectrolyte-Coated Liquid Crystal Droplets. *MSCE* **2014**, *2*, 1-7
- 50. Adam, C. J.; Clark, S. J.; Ackland, G. J.; Crain, J., Conformation-Dependent Dipoles of Liquid Crystal Molecules and Fragments from First Principles. *Phys. Rev. E.* **1997**, *55* (5), 5641-5649.
- 51. Bogi, A.; Faetti, S., Elastic, Dielectric and Optical Constants of 4'-Pentyl-4-Cyanobiphenyl. *Liq. Cryst.* **2010**, *28* (5), 729-739.
- 52. Ono, H.; Shibata, K., Simple Determination of Thermal and Thermo-Optical Constants of Liquid Crystals by Means of a Photothermal Self-Diffracting Technique. *Jpn. J. Appl. Phys.* **2003**, 42 (1), 186-193.
- 53. Bera, T.; Deng, J.; Fang, J., Protein-Induced Configuration Transitions of Polyelectrolyte-Modified Liquid Crystal Droplets. *J. Phys. Chem. B* **2014**, *118*, 4970-4975.
- 54. Chernyshuk, S. B.; Lev, B. I., Theory of Elastic Interaction of Colloidal Particles in Nematic Liquid Crystals Near One Wall and in the Nematic Cell. *Phys. Rev. E* **2011**, *84*, 011707.
- 55. Mustin, B.; Stoeber, B., Single Layer Deposition of Polystyrene Particles on to Planar Polydimethylsiloxane Substrates. *Langmuir* **2015**, *32*, 88-101.
- 56. Brown, M. A.; Abbas, Z.; Kleibert, A.; Green, R. G.; Goel, A.; May, S.; Squires, T. M., Determination of Surface Potential and Electrical Double-Layer Structure at the Aqueous Electrolyte-Nanoparticle Interface. *Phys. Rev. X* **2016**, *6*, 011007.

- 57. Herminghaus, S.; Maass, C. C.; Kruger, C.; Thutupalli, S.; Goehring, L.; Bahr, C., Interfacial Mechanisms in Active Emulsions. *Soft Matter* **2014**, *10*, 7008-7022.
- 58. Nery-Azevedo, R.; Banerjee, A.; Squires, T. M., Diffusiophoresis in Ionic Surfactant Gradients. *Langmuir* **2017**, *33*, 9694-9702.
- 59. Prieve, D. C.; Malone, S. M.; Khair, A. S.; Stout, R. F.; Kanj, M. Y., Diffusiophoresis of Charged Colloidal Particles in the Limite of Very High Salinity. *PNAS* **2018**, *116* (37), 18257-18262. 60. Shah, R. R.; Abbott, N. L., Coupling of the Orientations of Liquid Crystals to Electrical Double Layers Formed by the Dissociation of Surface-Immobilized Salts. *J. Phys. Chem. B* **2001**, *105*, 4936-4950.
- 61. Noh, J.; Sousa, K. R. D.; Lagerwall, J. P. F., Influence of Interface Stabilisers and Surrounding Aqueous Phases on Nematic Liquid Crystal Shells. *Soft Matter* **2016**, *12* (2), 367-372.
- 62. Yazdi, A. S., Surfactant-Based Extraction Methods. *Trends Analyt. Chem.* **2011**, *30* (6), 918-929.
- 63. Rumyantsev, A. M.; Santer, S.; Kramarenko, E. Y., Theory of Collapse and Overcharging of a Polyelectrolyte Microgel Induced by an Oppositely Charged Surfactant. *Macromolecules* **2014**, *47*, 5388-5399.
- 64. Guzman, E.; Llamas, S.; Maestro, A.; Fernandez-Pena, L.; Akanno, A.; Miller, R.; Ortega, F.; Rubio, R. G., Polymer-Surfactant Systems in Bulk and at Fluid Interfaces. *Adv. Colloid Interface Sci.* **2016**, *233*, 38-64.
- 65. Taylor, D. J. F.; Thomas, R. K.; Penfold, J., Polymer/Surfactant Interactions at the Air/Water Interface. *Adv. Colloid Interface Sci.* **2007**, *132*, 69-110.
- 66. Varga, I.; Campbell, R. A., General Physical Description of the Behavior of Oppositely Charged Polyelectrolyte/Surfactant Mixtures at the Air/Water Interface. *Langmuir* **2017**, *33* (23), 5915-5924.
- 67. Prelesnik, S.; Larin, S.; Aseyev, V.; Tenhu, H.; Kogej, K., Water-Soluble Nonstoichiometric Complexes Between Sodium Poly(styrenesulfonate) and Cetylpyridinium Chloride in Aqueous NaCl Solutions. A Static and Dynamic Light Scattering Study. *J. Phys. Chem. B.* **2011**, *115*, 3793-3803.
- 68. Kogej, K., Association and Structure Formation in Oppositely Charged Polyelectrolyte-Surfactant Mixtures. *Adv. Colloid Interface Sci.* **2010**, *158*, 68-83.
- 69. Lee, J.; Moroi, Y., Investigation of the Interaction between Sodium Dodecyl Sulfate and Cationic Polymers. *Langmuir* **2004**, *20*, 4376-4379.

- 70. Lapitsky, Y.; Parikh, M.; Kaler, E. W., Calorimetric Determination of Surfactant/Polyelectrolyte Binding Isotherms. *J. Phys. Chem. B* **2007**, *111*, 8379-8387.
- 71. Schabes, B. K.; Richmond, G. L., Helping Strands: Polyelectrolyte Assists in Surfactant Assembly Below Critical Micelle Concentration. *J. Phys. Chem. B* **2020**, *124* (1), 234-239.
- 72. Tong, L. J.; Bao, M. T.; Li, Y. M.; Gong, H. Y., Interfacial Dynamic and Dilational Rheology of Polyelectrolyte/Surfactant Two-Component Nanoparticle Systems at Air-Water Interface. *Appl. Surf. Sci.* **2014**, *316*, 147-154.
- 73. Bergeron, V.; Langevin, D.; Asnacios, A., Thin-Film Forces in Foam Films Containing Anionic Polyelectrolyte and Charged Surfactants. *Langmuir* **1996**, *12* (6), 1550-1556.
- 74. Langevin, D., Polyelectrolyte and Surfactant Mixed Solutions. Behavior at Surfaces and in Thin Films. *Adv. Colloid Interface Sci.* **2001**, *89-90*, 467-484.
- 75. Tan, L. N.; Orler, V. J.; Abbott, N. L., Ordering Transitions Triggered by Specific Binding of Vesicles to Protein-Decorated Interfaces of Thermotropic Liquid Crystals. *Langmuir* **2012**, *28* (15), 6364-6376.
- 76. Tercero, M. D. D.; Abbott, N. L., Ordering Transitions in Liquid Crystals Permit Imaging of Spatial and Temporal Patterns Formed by Proteins Penetrating into Lipid-Laden Interfaces. *Chem. Eng. Sci.* **2008**, *196* (12), 234-251.
- 77. Brake, J. M.; Daschner, M. K.; Abbott, N. L., Formation and Characterization of Phospholipid Monolayers Spontaneously Assembled at Interfaces between Aqueous Phases and Thermotropic Liquid Crystals. *Langmuir* **2005**, *21*, 2218-2228.
- 78. Verma, I.; Lekshmy, S.; Selvakumar, V.; Pal, S. K., Surfactin-Laden Aqueous-Liquid Crystal Interface Enabled Identification of Secondary Structure of Proteins. *J. Phys. Chem. C.* **2020**, *124*, 780-788.
- 79. Monteux, C.; Williams, C. E.; Meunier, J.; Anthony, O.; Bergeron, V., Adsorption of Oppositely Charged Polyelectrolyte/Surfactant Complexes at the Air/Water Interface: Formation of Interfacial Gels. *Langmuir* **2004**, *20*, 57-63.
- 80. Monteux, C.; Fuller, G. G.; Bergeron, V., Shear and Dilational Surface Rheology of Oppositely Charged Polyelectrolyte/Surfactant Microgels Adsorbed at the Air-Water Interface. Influence on Foam Stability. *J. Phys. Chem. B* **2004**, *108* (42), 16473-16482.

## **Table of Contents Graphic**

